Eur. Phys. J. C (2013) 73:2313
DOI 10.1140/epjc/s10052-013-2313-1

THE EUROPEAN PHYSICAL JOURNAL C

Special Article - Tools for Experiment and Theory

Ascertaining the spin for new resonances decaying into $\tau^+\tau^-$ at hadron colliders

S. Banerjee[1], **J. Kalinowski**[2,a], **W. Kotlarski**[2], **T. Przedzinski**[3], **Z. Wąs**[4,5]

[1]Department of Physics, University of Wisconsin, Madison, WI 53706, USA
[2]Faculty of Physics, University of Warsaw, ul. Hoża 69, Warsaw, Poland
[3]Faculty of Physics, Astronomy and Applied Computer Science, Jagellonian University, Reymonta 4, 30-059, Kraków, Poland
[4]Institute of Nuclear Physics, PAN, ul. Radzikowskiego 152, Kraków, Poland
[5]CERN PH-TH, 1211 Geneva 23, Switzerland

Received: 31 December 2012 / Revised: 31 January 2013 / Published online: 13 February 2013

Abstract Evidence of a new particle with mass ∼125 GeV decaying into a pair of tau leptons at the Large Hadron Collider spurs interest in ascertaining its spin in this channel. Here we present a comparative study between spin-0 and spin-2 nature of this new particle, using spin correlations and decay product directions. The `TauSpinner` algorithm is used to re-weight distributions from $q\bar{q} \to \gamma/Z \to \tau^+\tau^-$ sample to simulate a spin-2 state exchange. The method is based on supplementing the Standard Model matrix elements with those arising from presence of a new interaction. Studies with simulated samples demonstrate the discrimination power between these spin hypotheses based on data collected at the Large Hadron Collider.

1 Introduction

Following the discovery of a Higgs-like state H with mass ∼125 GeV at the Large Hadron Collider (LHC) [1, 2], its spin-parity assignment must be examined to verify the true nature of this new state. The spin of this newly observed state has recently been discussed [3–7] in the context of its couplings to a pair of vector bosons. However, from an experimental point of view, the spin property should be investigated channel by channel, and other alternative hypotheses should be investigated and excluded. At the HCP'12 conference, the ATLAS [8] and the CMS [9] collaborations reported observed significances of 1.1 σ and 1.5 σ respectively, for the $H \to \tau^+\tau^-$ decay channel. Their corresponding expected significances are 1.7 σ and 2.5 σ, which when added in quadrature are already at the 3 σ level. In the present paper, we concentrate on this channel as a possible completion of the spin studies.

Searches for $H \to \tau^+\tau^-$ decay are challenging because the τ neutrino's escape detection. Experimental signatures are categorized over multiple channels in terms of observable final state decay products. Data from the multi-channel inputs must be compared with simulation of large samples of Monte Carlo (MC) events, which includes detector resolution and acceptance effects, as well as contributions from background events in the selected sample.

The study of τ polarization can provide additional leverage for this search. The `TauSpinner` algorithm [10] provides a mechanism for evaluating the polarization effects of τ spin. The algorithm based on the re-weighting technique can be applied to the existing sample of simulated MC events, thereby reducing the need for computationally intensive simulation of independent samples, and has successfully been applied for measurements of τ polarization in $W^\pm \to \tau^\pm\nu$ [11] and $Z \to \tau^+\tau^-$ [12] decays.

In the present paper we extend the method of `TauSpinner` by adding contributions from new resonances to the amplitude of $q\bar{q} \to \gamma/Z \to \tau^+\tau^-$ processes. Our numerical study based on exchange of a spin-2 state X is motivated by recent interest in measurement of spin properties for the newly discovered Higgs-like particle candidate. In general, contribution from other new interactions, such as those arising from an additional Z' boson, can also be evaluated in this way. Though the present implementation illustrates re-weighting of samples generated with Pythia [13], the method is equally applicable to other MC event generators.

Our paper is organized as follows. In the next section we discuss contributions from spin-2 state to the matrix element. Section 3 is devoted to the `TauSpinner` algorithm and the inclusion of new matrix elements into the program. Section 4 is devoted to technical tests of the `TauSpinner` algorithm and stability tests of internal cross-checks. In

[a] e-mail: jan.kalinowski@fuw.edu.pl

Sect. 5, we investigate experimentally discriminating variables sensitive to spin. In Sect. 6, we perform a numerical analysis to access the sensitivity to measure the spin properties of Higgs-like states. Section 7 presents the Summary and Appendix closes the paper with a detailed description of updates to the `TauSpinner` algorithm.

2 Quark level cross section for $\gamma/Z/X$ production of tau pairs

In many theoretical models massive objects of spin-2 arise, including KK gravitons [14–16], analogues of the f_2 state of QCD in a new strongly-interacting sector [17] or states in four-dimensional ghost-free models of massive gravity [18]. For our purposes we will treat the spin-2 particle with mass of 125 GeV as a low-energy signature of some unspecified high-energy completion of the model. Therefore, we will use an effective Lagrangian formalism for a spin-2 field interacting with fermions to calculate the angular distribution in the process $q\bar{q} \to \gamma/Z/X \to \tau^+\tau^-$ at the lowest level. These quark level calculations are implemented in the `TauSpinner` [10] algorithm, as described in Sect. 3.

For a symmetric spin-2 field $X_{\mu\nu}$ with mass M_X, decay width Γ_X and momentum k the propagator reads [19] as:

$$\Delta^{\mu\nu,\alpha\beta}(k) = \frac{i P^{\mu\nu,\alpha\beta}}{k^2 - M_X^2 + i M_X \Gamma_X}. \tag{1}$$

The projector P is given by:

$$P^{\mu\nu,\alpha\beta} = \frac{1}{2}\left(\eta^{\mu\alpha}\eta^{\nu\beta} + \eta^{\mu\beta}\eta^{\nu\alpha}\right) - \frac{1}{3}\eta^{\mu\nu}\eta^{\alpha\beta} + \cdots, \tag{2}$$

where $\eta^{\mu\nu}$ is the Minkowski tensor. The terms proportional to the momentum k, represented by dots in the above formula, will vanish when contracted with the on-shell massless fermion currents.

The interactions of $X^{\mu\nu}$ with fermions consists of various operators of increasing dimensions, suppressed by powers of some high scale denoted by F. At zero derivative level the coupling of X to a fermion current has a form:

$$\mathcal{L} \ni X_\mu^\mu \bar{\psi}(\lambda_L P_L + \lambda_R P_R)\psi + h.c., \tag{3}$$

where $P_{L,R} = (1 \mp \gamma_5)/2$. This form of coupling is similar to an ordinary Yukawa coupling of a Standard Model (SM) singlet scalar. Therefore its experimental signatures: angular distributions and spin correlations, will be similar to a scalar exchange, with the only difference coming from the spin-2 propagator. If the $X^{\mu\nu}$ were of gravity or extra dimension origin, the couplings λ_i for light fermions would naturally be suppressed by the fermion mass, $\lambda \sim m/F$. Therefore, in the discussion of the τ-lepton pair production via Drell–Yan process in pp collisions such couplings will be ignored.

At dimension 5 level the coupling of $X^{\mu\nu}$ to a fermion bilinear is given by [20–23]:

$$\begin{aligned}\mathcal{L} \ni \frac{i}{4}\frac{1}{F} X^{\mu\nu}\big[&\alpha^L \bar{\psi}_L(\gamma_\mu\partial_\nu + \gamma_\nu\partial_\mu)\psi_L \\ &+ \beta^L(\partial_\nu\bar{\psi}_L\gamma_\mu + \partial_\mu\bar{\psi}\gamma_\nu)\psi_L\big] \\ &+ (L \to R) + h.c.\end{aligned} \tag{4}$$

Other possible dimension 5 couplings $\sim X_\mu^\mu \bar{\psi}\partial\!\!\!/\psi$ will be ignored since for the on-shell fermions they can be reduced to the form in Eq. (3).

The couplings $\alpha^{L,R}, \beta^{L,R}$ are model-dependent. Although we do not attempt to construct any specific model, we assume that the couplings are quark- and lepton-flavor diagonal and, following Ref. [23], we make a simplifying assumption:

$$\alpha^{L,R} = -\beta^{L,R} \equiv g^{L,R}. \tag{5}$$

At tree level the process $q\bar{q} \to \tau^+\tau^-$ proceeds via s-channel $\gamma/Z/X$ exchanges. Let g^i_{Aff} (with $i = L, R$) denote the chiral couplings of $A = \gamma, Z, X$ bosons to a fermion current $\bar{f}f$. In particular, for SM couplings we have $g^i_{\gamma ff} = eQ_f$, $g^i_{Zff} = \frac{g}{\cos\theta_W}(T_f^3 - Q_f \sin^2\theta_W)$, with g weak coupling constant, and eQ_f, T_f^3 are the fermion electric charge and third component of weak isospin. We also introduce a short-hand notation $\gamma_{ij} \equiv g^i_{\gamma qq} g^j_{\gamma\tau\tau}$, $Z_{ij} \equiv g^i_{Zqq} g^j_{Z\tau\tau}$, and $X_{ij} \equiv g^i_{Xqq} g^j_{X\tau\tau}$. The angular distribution in the CM frame can then be written as a sum of the SM contribution:

$$\begin{aligned}\frac{d\sigma^{SM}}{d\cos\theta} = &\frac{1}{384\pi s}\big[(\gamma_{LL}^2 + \gamma_{RR}^2)(1+\cos\theta)^2 \\ &+ (\gamma_{LR}^2 + \gamma_{RL}^2)(\cos\theta - 1)^2\big] \\ &- \frac{1}{192\pi}\frac{(M_Z^2 - s)}{(M_Z^2 - s)^2 + M_Z^2\Gamma_Z^2} \\ &\times \big[(\gamma_{LL}Z_{LL} + \gamma_{RR}Z_{RR})(1+\cos\theta)^2 \\ &+ (\gamma_{LR}Z_{LR} + \gamma_{RL}Z_{RL})(\cos\theta - 1)^2\big] \\ &+ \frac{1}{384\pi}\frac{s}{(M_Z^2 - s)^2 + M_Z^2\Gamma_Z^2} \\ &\times \big[(Z_{LL}^2 + Z_{RR}^2)(1+\cos\theta)^2 \\ &+ (Z_{LR}^2 + Z_{RL}^2)(\cos\theta - 1)^2\big]\end{aligned} \tag{6}$$

and a new term from the X particle exchange, including its interference with the SM contribution. For a real field X and real couplings g^i_{Xff} it reads:

$$\begin{aligned}\frac{d\sigma^X}{d\cos\theta} = &\frac{1}{24576\pi F^4}\frac{s^3}{(M_X^2 - s)^2 + M_X^2\Gamma_X^2} \\ &\times \big[(X_{LL}^2 + X_{RR}^2)\big(-1 + 2\cos^2\theta + \cos\theta\big)^2\end{aligned}$$

$$
\begin{aligned}
&+\left(X_{LR}^2+X_{RL}^2\right)\left(1-2\cos^2\theta+\cos\theta\right)^2\Big] \\
&-\frac{1}{1536\pi F^2}\,\frac{s(M_X^2-s)}{(M_X^2-s)^2+M_X^2\Gamma_X^2} \\
&\times\Big[\left(\gamma_{LL}X_{LL}+\gamma_{RR}X_{RR}\right)f_1(\theta) \\
&+\left(\gamma_{LR}X_{LR}+\gamma_{RL}X_{RL}\right)f_2(\theta)\Big] \\
&+\frac{1}{1536\pi F^2} \\
&\times\frac{s^2((M_Z^2-s)(M_X^2-s)+M_Z\Gamma_Z M_X\Gamma_X)}{((M_Z^2-s)^2+M_Z^2\Gamma_Z^2)((M_X^2-s)^2+M_X^2\Gamma_X^2)} \\
&\times\Big[\left(Z_{LL}X_{LL}+Z_{RR}X_{RR}\right)f_1(\theta) \\
&+\left(Z_{LR}X_{LR}+Z_{RL}X_{RL}\right)f_2(\theta)\Big]. \qquad (7)
\end{aligned}
$$

In the above expressions θ is the CM scattering angle of τ^- with respect to the incoming quark momentum, and $f_1(\theta)=(1+\cos\theta)^2(2\cos\theta-1)$ and $f_2(\theta)=(1+2\cos\theta)(\cos\theta-1)^2$.

The angular distribution due to the X state exchange depends on its couplings. For general chiral couplings, the diagonal term is a fourth order polynomial in $\cos\theta$, and the interference a third order polynomial. For vector or axial-vector type couplings ($g^L_{Xff}=\pm g^R_{Xff}$), the expressions in Eq. (7) simplify and the diagonal term exhibits a well known angular distribution $1-3\cos^2\theta+4\cos^4\theta$, while the interference with the SM contribution behaves as $\cos^3\theta$ and vanishes after angular integration. This can be observed in Fig. 6 discussed later in the paper. For general couplings the interference survives the angular integration.

The user may take his/her preferred scenario and modify the parameters, including the SM ones, in these new currents. For the sake of numerical comparisons, we use $F=1000$ GeV to study the effects of the spin-2 state X at 125 GeV. The width of this state is taken to be 1.5 GeV.

Unless otherwise mentioned, for the default comparison, we set both the left-handed and right-handed couplings to have the strengths of unity. We also study two alternative scenarios of pure left-handed or pure right-handed couplings labeled in subsequent discussions as L and R respectively. For these alternative models, the non-vanishing coupling constants are increased by $\sqrt{2}$ to allow direct comparison with the model (L+R) where both couplings contribute equally.

3 Algorithm case of non-standard model weight

Basic functionality of `TauSpinner` relies on the calculation of effective Born cross sections. It is documented in detail in Ref. [10]. For the extension of the `TauSpinner` algorithm, starting with the case of production of $q\bar{q}\to\gamma/Z\to\tau^+\tau^-$ events, we replace the effective Born level contribution with the one where amplitudes due to the extra interaction are added. At present, the algorithm assumes that the resulting new cross-section has contributions from polynomials at most of the 4th order in *cosine* of the scattering angle θ. Spin correlations between the produced τ^+ and τ^- remain as in the case of γ/Z production, but differ only in angular dependence of the τ polarization. Thus, the non-Standard Model weight can easily be calculated using the algorithm described in Appendix B.2 of [10]. With minor modifications as interfaced with the `Tauola++` MC event generator [24], the algorithm is described below:

- Initialize `Tauola++`
- Initialize `TauSpinner`
  At this step, user provides two additional flags, `nonSM2` and `nonSMN`. The first one activates calculation of non-Standard Model weight. Then effects due to spin correlations, described by the ratio of `WT1` and `WT2`,[1] and effects on angular dependence in $\tau^+\tau^-$ production are introduced with `WT3`. The factor due to the ratio of angle-integrated cross-section of the SM and nonSM case is removed from `WT3` if `nonSMN` is set to 1. All other aspects of `TauSpinner` remain unchanged.
- Read the data files
- Calculate the weights
  For the new non-Standard Model case, this step is extended:
  - As in default case, calculate spin weight `WT1` for Standard Model spin correlations
  - Calculate spin weight `WT2` for spin correlations calculated in non-Standard Model case. Use `setNonSMkey(1)` to switch to non-Standard Model calculation mode.
  - Calculate non-Standard Model weight `WT3` for effects on cross section; use `double getWtNonSM()` for its calculation.
  - return `WT = (WT2/WT1) * WT3`

An example of such a calculation is given in our `taureweight-text.cxx`. Weight calculation is prepared for the case when the generated sample has already the SM spin correlations taken into account. User is free to use his/her own version of the function providing the Born level τ pair production and featuring another assumptions for the SM extension. The necessary methods are described in Appendix.

4 Technical tests

Before any use of our program is started, some technical tests must be performed to verify if the function used in the

[1] `WT1` is the spin weight of Standard Model and `WT2` is when non-Standard Model interactions are switched on. `WT1` is the default spin weight that `TauSpinner` returns.

implementation of the non-Standard Model interaction is proper from the point of view of our program requirements. The first is to check the user provided non-Standard Model Born cross-section. In particular, it has to be checked that the same conventions for input parameters as those used in TauSpinner and Tauola++ are chosen. In our case, for the model as described in previous sections, adjustment of signs for spin states had to be introduced. The C++ function nonSM_adopt is prepared for the adjustment of conventions.

An arrangement to verify the proper matching is prepared (overall s-dependent factors cancel out). Special printouts from TAUOLA/TauSpinner/src/spin2.cxx are activated in the DEBUG mode of TauSpinner. Comparison of τ polarization calculated from the TauSpinner default implementation and the ones from user prepared inputs are then printed. The corresponding DEBUG mode printout looks as follows:

```
test of nonSM Born nonsm2=0
ide,svar,costhe=1 292.05 0.74348
sm=0.529759 sm(new)=0.530185 nsm=0.530185
sm and sm(new) should be essentially equal.
```

The sm and sm(new) denote τ polarization as obtained from the Standard Model respectively by the method of TauSpinner and the one of the user (the third quantity, nsm, provided by the user includes additional interaction, which for $\texttt{svar} = s = 292.05\ \text{GeV}^2$ is consistent with zero).

Graphic representations of the above tests are provided in Fig. 1 as a function of $\sqrt{s}$ for a fixed scattering angle θ, and in Fig. 2 for fixed $\sqrt{s}$ and as a function of θ. In Fig. 1 consistency up to per mille level on the τ polarization is obtained by replacing the TauSpinner standard method of Born calculation with the one as defined in Sect. 2. For nonSM2=0 agreement between the user method and TauSpinner default should be obtained as in our case. This is necessary to ensure that the non Standard model effect can be correctly implemented with nonSM2=1. In Fig. 2, distributions from all SM contribution as well as new contributions to the τ polarization are superimposed on the same figure. Good enough agreement demonstrates the validity of this technical test. Further fine tuning of pa-

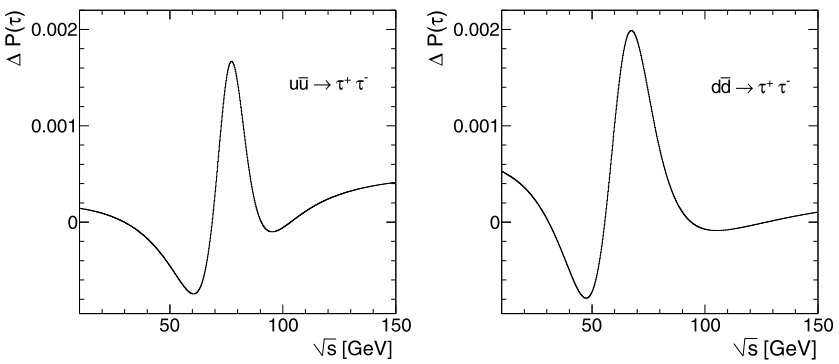

Fig. 1 The difference between the τ polarization calculated analytically from formulae as described in Sect. 2 but with new effects switched off, and the default implementation in the Tauola++ are plotted for fixed scattering angle $\cos\theta = 0.3$ as a function of $\sqrt{s}$. The *plot on the left* is for up quarks, and the *plot on the right* is for down quarks

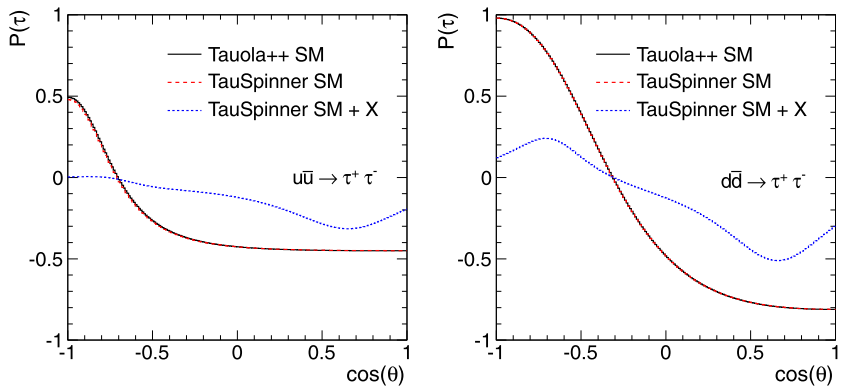

Fig. 2 Angular dependence of the τ polarization in the rest frame of hard process is shown for virtuality fixed at 125 GeV, for up quarks *on the left plot* and down-quarks *on the right plot*. The *black solid line* is the SM contribution from default implementation in Tauola++, and the *red dashed line* is the SM contribution but using the nonSM package. The effect of nonSM interaction is also shown on the same plots by the *blue dotted lines* (Color figure online)

Table 1 Average τ polarization for the SM and non-SM contributions as calculated from helicity states attributed by standard `TauSpinner` method `getTauSpin()`

Selection	$Z \to \tau^+\tau^-$	$Z/X(\mathrm{L}+\mathrm{R}) \to \tau^+\tau^-$
125 ± 3 GeV	-0.448 ± 0.001	-0.354 ± 0.001
`WT - 1`	–	-0.255 ± 0.001
Selection	$Z/X(L) \to \tau^+\tau^-$	$Z/X(R) \to \tau^+\tau^-$
125 ± 3 GeV	-0.521 ± 0.001	-0.071 ± 0.001
`WT - 1`	-0.574 ± 0.001	0.130 ± 0.001

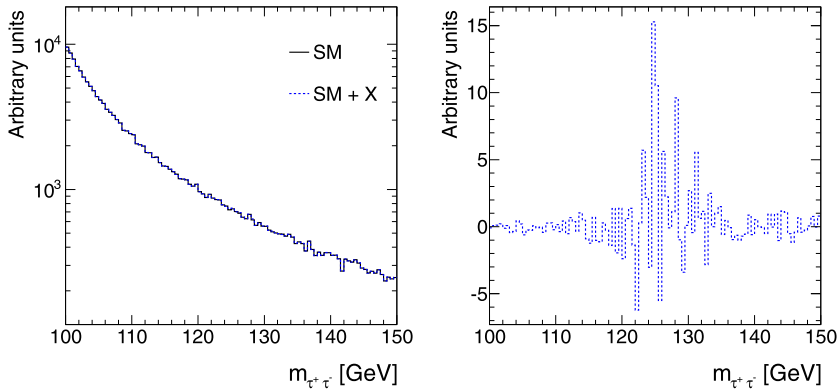

Fig. 3 Distributions of invariant masses of the τ pair are shown for the SM contribution in *solid black line on the left plot*. The almost overlapping *dotted blue line* includes the effect from non-SM contribution, but angular integration dependent contributions to the cross section are removed from the weight. The *right hand side plot* visualizes the difference, obtained by applying a weight = `WT - 1` (Color figure online)

rameters and schemes (e.g. constant or running Z width) in `Tauola++` is not necessary.[2]

Table 1 represents further tests of τ polarization, where we check that proper spin states of τ are provided by the `TauSpinner` algorithm using the `getTauSpin()` method (see Ref. [10] for definition). Average τ polarizations are shown when the virtuality of τ pair is required to lie within a ± 3 GeV window centered around 125 GeV in the top row. For the bottom row, a weight = `WT - 1` is used instead of the cut on virtuality. Nonetheless, the τ polarization still includes contributions from the SM via the interference effects between the SM and non-SM interactions. The following cases are monitored: in the upper part of the table the SM contribution (second column), non-SM contributions for the case of (L+R) couplings as in Sect. 2 (third column), and in the lower part of the table only left coupling for non SM (second column) and only right couplings (third column). The use of the weight = `WT - 1` is of interest for study of dedicated sub-samples.

Second test is performed to check the implementation of non-SM effects when dependence of the cross-section on τ angular distribution and spin effects are included, but those arising from integrated Born level cross section are removed. In the `TauSpinner` algorithm, we integrate the distribution over $\cos\theta$ for the SM cross-sections at the Born level and calculate the effect due to non-SM interactions. If the calculations are correct, these two contributions from the new matrix element should compensate each other in the distribution of τ pair invariant mass $m_{\tau^+\tau^-}$, as visible in Fig. 3. The black solid histogram describing the SM contribution in `TauSpinner` is taken by setting both the flags `nonSM2` and `nonSMN` to be equal to 0, whereas for the blue dotted line the new current from `TauSpinner` is used but its effects on the cross section are removed. It is tested by setting both flags, `nonSM2` and `nonSMN`, to be equal to 1. Change of angular distributions resulting from the weight, but integrated over $\cos\theta$, results in increased statistical fluctuations as visible on the right hand plot in Fig. 3 obtained using weight = `WT - 1`. The amplitude of this procedure is consistent with zero up to per mille level, as expected from the size of agreement observed in Fig. 1.

The differential effect of not integrating over the angular dependence due to non-SM interactions recovers the expected peaking structure around 125 GeV as shown in the red dashed histograms in Fig. 4, which are obtained by setting the flags `nonSM2` and `nonSMN` to be equal to 1 and 0, respectively.

5 Spin sensitive observables

The main feature of `TauSpinner` is that it can work on previously generated and stored data files of the simulated events. For our purposes, we study $pp \to Z \to \tau^+\tau^-$ generated at $\sqrt{s} = 8$ TeV using `Pythia8` [13] MC generator, with τ decays simulated by `Tauola++` [24]. To apply

[2] One has to bear in mind that `TauSpinner` constructs the hard process kinematic configuration differently than `Tauola++`. See Ref. [10] for discussion of potential but minor systematic errors.

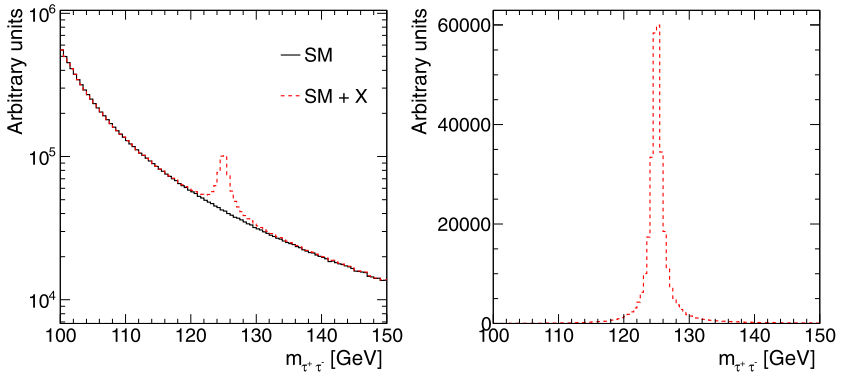

Fig. 4 Distributions of invariant masses of the τ pair are shown for the SM contribution in *solid black line on the left plot*. The *dashed red line* includes the effect from non-SM contribution. The *right hand side plot* visualizes the difference, obtained by applying a weight = `WT - 1` (Color figure online)

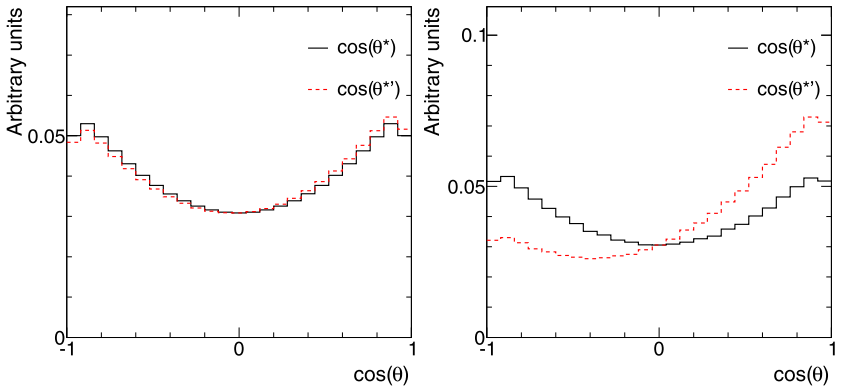

Fig. 5 The distributions of $\cos(\theta^\star)$ and $\cos(\theta^{\star\prime})$ variables are shown for $Z \to \tau^+\tau^-$ events before any cuts (*on the left*) and cuts on truth level invariant mass of the $\tau^+\tau^-$ system restricted to lie within a ± 3 GeV window centered around 125 GeV (*on the right*). All distributions are normalized to unit area (Color figure online)

non-Standard Model weight, `TauSpinner` was used.[3] The distributions for $X \to \tau^+\tau^-$ are obtained by re-weighting the corresponding distributions from $Z \to \tau^+\tau^-$ samples with weight = `WT - 1`. The samples for gluon-gluon fusion and vector-boson fusion production of the Higgs are generated using `POWHEG-BOX` [25, 26] MC generator interfaced to `Pythia8` for showering and hadronization, while `Pythia8` is used for the vector-boson associated Higgs production. The sample of $H \to \tau^+\tau^-$ events are obtained by summing these three samples weighted by their respective cross-sections [27, 28].

We study the variable $\cos(\theta^\star)$ [29], describing the average scattering angle between the observable final state products from τ^+ and τ^- decays, respectively. In the leading approximation, it corresponds to the scattering angle in the rest-frame of hard process. In the laboratory frame, this variable is defined as:

$$\cos\left(\theta^\star\right) = \frac{\sin\theta^{\tau^-}\cos\theta^{\tau^+} + \sin\theta^{\tau^+}\cos\theta^{\tau^-}}{\sin\theta^{\tau^+} + \sin\theta^{\tau^-}}, \tag{8}$$

where θ^{τ^+} is the angle between the decay products from τ^+ and negative z-axis, and θ^{τ^-} is the angle between the decay products from τ^- and positive z-axis.

[3]From `Tauola++` version `v1.1.0`, `TauSpinner` is provided as a part of the `Tauola++` distribution.

Sensitivity to forward-backward asymmetry is enhanced by flipping the sign of the variable $\cos(\theta^\star)$, whenever the vector sum of momentum of the visible τ daughters is aligned towards the negative z-axis. This defines the variable $\cos(\theta^{\star\prime})$, which is sensitive to the spin of $Z/X/H$.

The distributions of $\cos(\theta^\star)$ and $\cos(\theta^{\star\prime})$ are shown in Fig. 5 for $Z \to \tau^+\tau^-$ events. The left plot in Fig. 5 compares the distributions before any cuts. The right plot compares the distributions after a cut on virtuality has been applied by selecting events with the truth level invariant mass of the $\tau^+\tau^-$ system restricted to lie within a ± 3 GeV window centered around 125 GeV.

The distributions of $\cos(\theta^{\star\prime})$ for $X \to \tau^+\tau^-$, and $H \to \tau^+\tau^-$ events are shown on the left plot in Fig. 6. The effect of spin is clearly visible in this variable which shows striking difference as compared to $Z \to \tau^+\tau^-$ events, also shown in the same plot. The virtuality of all these processes is chosen to lie within a ± 3 GeV window centered around 125 GeV by applying a cut on the truth level invariant mass of the $\tau^+\tau^-$ system.

For the same selection criteria, the distribution of $X \to \tau^+\tau^-$ events are shown on the right plot in Fig. 6 for different choices of coupling constants. As expected from Table 1, the asymmetry in this variable is the strongest for the case of pure left-handed coupling, and the weakest for the case of pure right-handed coupling.

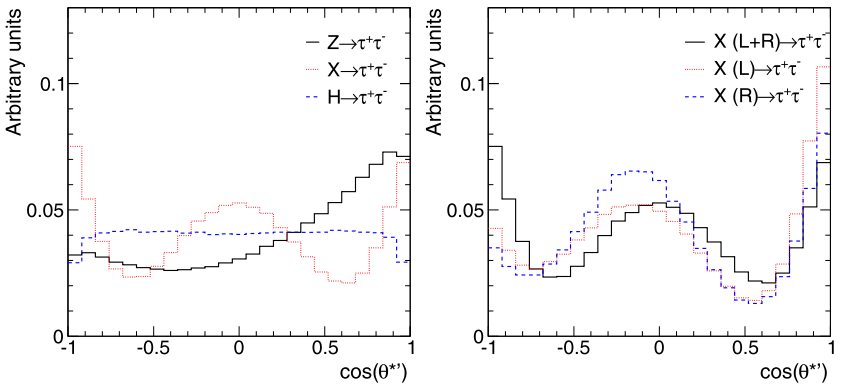

Fig. 6 The distributions of $\cos(\theta^{\star\prime})$ are shown for $Z \to \tau^+\tau^-$, $X \to \tau^+\tau^-$, and $H \to \tau^+\tau^-$ events after cuts on truth level invariant mass of the $\tau^+\tau^-$ system restricted to lie within a ± 3 GeV window centered around 125 GeV (*on the left*). For the same selection criteria, the distributions of $\cos(\theta^{\star\prime})$ are shown (*on the right*) for $X \to \tau^+\tau^-$ events for three choices of coupling constants as described in the text. All distributions are normalized to unit area (Color figure online)

6 Test for spin of $Z/X/H$

A key feature of τ polarization in $Z \to \tau^+\tau^-$ events is its dependence on virtuality of the hard interaction. To select the $Z \to \tau^+\tau^-$ events as relevant backgrounds for a Higgs-like particle with a mass of 125 GeV, we select events inside an appropriate window on the collinear mass ($m^{\text{coll}}_{\tau^+\tau^-}$) reconstructed from the τ decay products [30]. This is sufficient for illustration purposes, and is comparable to computationally intensive techniques developed for di-tau mass reconstruction [31].

Our selection criteria are similar to the ones as in Ref. [32, 33], and those used by the ATLAS [8] and CMS [9] collaborations. The following requirements are applied to select a sample of events enriched with a new resonance produced at 125 GeV:

- p_{T} for each of the visible daughters of the tau's are required to be greater than 20 GeV and lie within an acceptance of $|\eta| < 2.5$,
- the missing transverse momentum ($E^{\text{miss}}_{\text{T}}$), defined as the p_{T} of the vector sum of the neutrinos' momentum, is required to be greater than 20 GeV,
- the transverse mass of the system comprising of $E^{\text{miss}}_{\text{T}}$ and the visible daughter with smaller p_{T} defined as $\sqrt{2 p_{\text{T}} E^{\text{miss}}_{\text{T}} (1 - \cos\Delta\phi)}$ is required to be less than 50 GeV, where $\Delta\phi$ is the angle between the directions of $E^{\text{miss}}_{\text{T}}$ and visible daughter with smaller p_{T} in the plane perpendicular to the beam direction,
- the cosine of the 3-dimensional opening angle between the two daughters is required to be greater than -0.9,
- the difference in azimuthal angles between the two daughters is required to be less than 2.9, and
- $m^{\text{coll}}_{\tau^+\tau^-}$ is required to lie within a ± 10 GeV window centered around 125 GeV.

The stability of the distribution of the discriminating variable $\cos(\theta^{\star\prime})$ for $Z \to \tau^+\tau^-$ events with respect to selected region of virtuality is studied in Fig. 7. The requirements on the window on $m^{\text{coll}}_{\tau^+\tau^-}$ is varied, keeping all the other above-mentioned selection requirements the same. The left plot corresponds to ± 10, ± 5 and ± 20 GeV windows centered around 125 GeV. The right plot corresponds to ± 10, ± 5 and ± 10 GeV windows centered around 125, 110 and 140 GeV, respectively. For the case when virtuality is centered around 125 GeV, the distributions are compatible, while the shape is

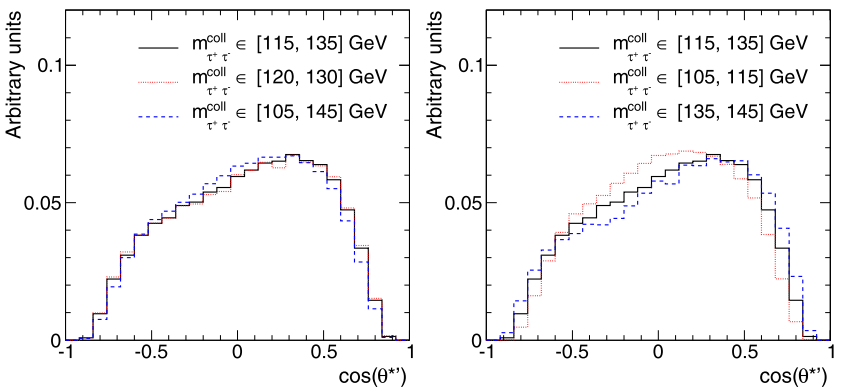

Fig. 7 The distributions of $\cos(\theta^{\star\prime})$ variable are shown for $Z \to \tau^+\tau^-$ events with cuts on reconstructed level quantity $m^{\text{coll}}_{\tau^+\tau^-}$. The *plot on the left* corresponds to ± 10, ± 5 and ± 20 GeV windows centered around 125 GeV. The *plot on the right* corresponds to ± 10, ± 5 and ± 5 GeV windows centered around 125, 110 and 140 GeV, respectively. All distributions are normalized to unit area (Color figure online)

altered with the shift of the center of the window. Thus, these differences in shapes can be taken as estimates of systematic uncertainties on the modeling of the background from $Z \to \tau^+\tau^-$ events.

The left plot in Fig. 8 shows the distribution of $\cos(\theta^{\star\prime})$ after applying these selection requirements to sample of $Z \to \tau^+\tau^-$, $X \to \tau^+\tau^-$, and $H \to \tau^+\tau^-$ events. For illustrative purposes, the distributions of $\cos(\theta^{\star\prime})$ are shown in the right plot of Fig. 8 for $X \to \tau^+\tau^-$ events passing criteria which correspond to the three different choices of the coupling constants.

Visible separation between the shapes of $H \to \tau^+\tau^-$ and $X \to \tau^+\tau^-$ events are observed, which is similar in size for all three choices of coupling constants studied. The distributions from $H \to \tau^+\tau^-$ events are incompatible at the 99 % confidence level with those arising from $X \to \tau^+\tau^-$ events for a sample of 500 Higgs-like events, which corresponds to roughly twice the number of signal events observed with 13 fb^{-1} at pp collision energy of 8 TeV by the ATLAS collaboration [8]. However, the separation power depends on the presence of backgrounds and choice of selection criteria, which alters relative efficiencies of signal and background events. Further discrimination power can be obtained by categorizing the $\tau^+\tau^-$ decay modes depending on the observed final state particles.

7 Summary

In this note we have presented a new development of the `TauSpinner` that is capable of addressing possible extension of the SM based on new physics model that results in contribution from a spin 2 state X. To simplify estimation of observability of such a state at the LHC, extension for the `TauSpinner` algorithm to manipulate τ pair final states in previously generated MC samples is proposed, which employs the method of event weights. Weights calculated with `TauSpinner` feature an implementation of amplitudes from beyond the Standard Model. Not only spin correlation effects as in the previous versions, but also effects modifying the angular distributions of $\tau^\pm$ lepton directions and size of the cross-section can be studied in this way.

An example of the installation of our new matrix elements into the `TauSpinner` algorithm is presented. Distributions validating correctness of the installation are discussed and found correct.

We then study distributions of experimentally observable quantities sensitive to the spin of $Z/X/H$. In semi-realistic conditions, we study the impact of the new interaction and its signature. We found the approximate hard process scattering angle $\theta^{\star\prime}$ reconstructed from observable directions of τ decay products to be useful for that purpose. Following the experimental searches performed with half the dataset expected to be collected at $\sqrt{s} = 8$ TeV in 2012, we apply selection criteria that enrich the sample of events with a Higgs-like state with mass ∼125 GeV. With double the number of Higgs-like events as can be expected using full 2012 dataset, we find distributions that are incompatible between $H \to \tau^+\tau^-$ and $X \to \tau^+\tau^-$ events at the 99 % confidence level. A detailed experimental study with all background contributions, which include detector resolution and acceptance effects, as categorized over the different $\tau^+\tau^-$ decay modes is expected to improve the discrimination power.

Robustness of the method was demonstrated here, and the first results are of potential interest. A key aspect of our `TauSpinner` algorithm is that computationally expensive simulation of independent MC samples is not necessary for study of new physics interactions. The method is also straightforward to extend to other cases such as Z' etc. Alternative production mechanisms of spin-2 states, e.g. via gluon-gluon fusion, vector-boson fusion etc., may also be implemented by inclusion of appropriate angular dependence from corresponding matrix elements in the user defined function. Re-weighting of the matrix elements from gluon-gluon fusion and vector-boson fusion processes will have to be then followed up by straightforward extensions of `TauSpinner` algorithm. This requires designing of new

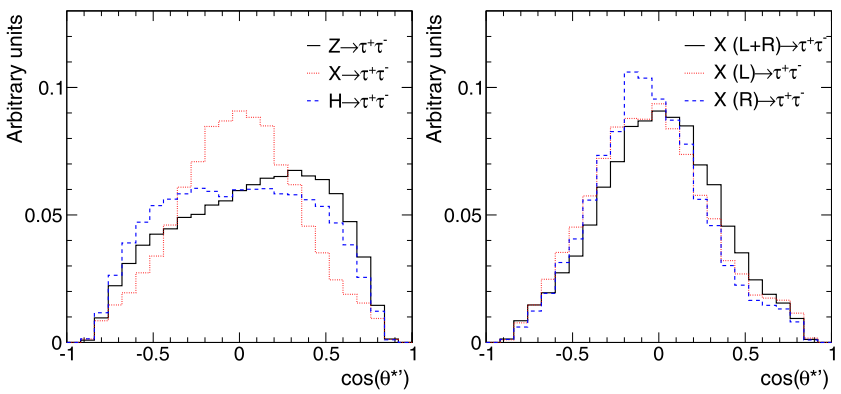

Fig. 8 The distributions of $\cos(\theta^{\star\prime})$ are shown (*on the left*) for $Z \to \tau^+\tau^-$, $X \to \tau^+\tau^-$, and $H \to \tau^+\tau^-$ events after cuts as described in the text. The distributions of $\cos(\theta^{\star\prime})$ are shown (*on the right*) after cuts for $X \to \tau^+\tau^-$ events with different options for coupling constants as described in the text. All distributions are normalized to unit area (Color figure online)

appropriate tests for validation of its functionality, to be reported in future publications. The sensitivity or the separation power between different spin hypotheses must then take into account the details of the event selection which would then result in different number of selected events and corresponding background categorization.

Acknowledgements Encouragement, support and discussions with Sau Lan Wu are acknowledged. Useful discussions with Ian Nugent are acknowledged. This project is financed in part from funds of Polish National Science Centre under decision DEC-2011/03/B/ST2/00107 (T.P.), DEC-2011/03/B /ST2/00220 (Z.W.) and DEC-2011/01/M/ST2/02466 (J.K.).

Appendix: `TauSpinner`—changes introduced in version 1.2

Since its first public version, described in [10], two new updates to `TauSpinner` have been introduced. First, `TauSpinner` has been merged into `Tauola++` [24] distribution and now, while working on this paper, it has been extended to add new functionality. In this section we list the changes between versions 1.0 and 1.2.

- Merging with `Tauola++`
  `TauSpinner` now comes as an additional library to `Tauola++` distribution. `Tauola++` configuration scripts have been updated to accommodate this setup. As of writing this paper, `Tauola++ v1.1.1`, featuring `TauSpinner v1.2` has been installed in database `GENSER` [34, 35].
- Two new initialization options - `nonSM2` and `nonSMN`
  The `nonSM2` flag turns on non-Standard Model weight calculation. The `nonSMN` flag, combined with `nonSM2`, allows for calculation of corrections to shape only.
- New functions added.
  Example `examples/tau-reweight-test.cxx` has been updated to show how functions described below can be used in case of spin-2 calculation described in this paper.
  - `set_nonSM_born(double (*fun)(int ID, double S, double cost, int H1, int H2, int key))`
    Sets function for user-defined Born, including new physics. The parameters of this new function are described in the file `include/TauSpinner/nonSM.h` as well as in the example program.
  - `void setNonSMkey(int key)`
    Sets the value of `nonSM2` flag. Allows turning non-Standard Model calculation on and off for comparison between different models.
  - `double getWtNonSM()` Returns non-Standard Model weight `WT3` calculated for the last event processed by `TauSpinner`.

In our `examples/tau-reweight-test.cxx` fortran function is provided to calculate quark level Born cross section where new physics effects can be switched on and off. Physics model described in the previous sections at the quark level annihilation into a pair of tau leptons is used. Function:

```
REAL*8 FUNCTION DISTJWK(ID,S,T,H1,H2,KEY)
```

is used in our program with the help of the C++ function:

```
double nonSM_adopt(int ID, double S,
double cost, int H1, int H2, int key)
```

Its use is initialized with the method

```
set_nonSM_born(nonSM_adopt);
```

Other user defined functions can be used in the same way.

References

1. ATLAS Collaboration, Phys. Lett. B **716**, 1–29 (2012). arXiv:1207.7214 [hep-ex]
2. CMS Collaboration, Phys. Lett. B **716**, 30–61 (2012). arXiv:1207.7235 [hep-ex]
3. S.Y. Choi, M.M. Muhlleitner, P.M. Zerwas, arXiv:1209.5268 [hep-ph]
4. J. Ellis, R. Fok, D.S. Hwang, V. Sanz, T. You, arXiv:1210.5229 [hep-ph]
5. J. Frank, M. Rauch, D. Zeppenfeld, arXiv:1211.3658 [hep-ph]
6. S. Bolognesi, Y. Gao, A.V. Gritsan, K. Melnikov, M. Schulze, N.V. Tran, A. Whitbeck, Phys. Rev. D **86**, 095031 (2012). arXiv:1208.4018 [hep-ph]
7. C. Englert, D. Goncalves-Netto, K. Mawatari, T. Plehn, arXiv:1212.0843 [hep-ph]
8. ATLAS Collaboration, ATLAS-CONF-2012-160
9. CMS Collaboration, CMS-PAS-HIG-12-043
10. Z. Czyczula, T. Przedzinski, Z. Was, Eur. Phys. J. C **72**, 1988 (2012). arXiv:1201.0117 [hep-ph]
11. G. Aad et al. (ATLAS Collaboration), Eur. Phys. J. C **72**, 2062 (2012). arXiv:1204.6720 [hep-ex]
12. I. Deigaard. MSc Thesis, University of Copenhagen. CERN-THESIS-2012-091
13. T. Sjostrand, S. Mrenna, P. Skands, Comput. Phys. Commun. **178**, 852–867 (2008). arXiv:0710.3820 [hep-ph]
14. N. Arkani-Hamed, S. Dimopoulos, G.R. Dvali, Phys. Lett. B **429**, 263 (1998). hep-ph/9803315
15. I. Antoniadis, N. Arkani-Hamed, S. Dimopoulos, G.R. Dvali, Phys. Lett. B **436**, 257 (1998). hep-ph/9804398
16. L. Randall, R. Sundrum, Phys. Rev. Lett. **83**, 3370 (1999). hep-ph/9905221
17. C.J. Morningstar, M.J. Peardon, Phys. Rev. D **56**, 4043 (1997). hep-lat/9704011
18. C. de Rham, G. Gabadadze, Phys. Lett. B **693**, 334 (2010). arXiv:1006.4367 [hep-th]

19. H. van Dam, M.J.G. Veltman, Nucl. Phys. B **22**, 397 (1970)
20. G.F. Giudice, R. Rattazzi, J.D. Wells, Nucl. Phys. B **544**, 3 (1999). hep-ph/9811291
21. T. Han, J.D. Lykken, R.-J. Zhang, Phys. Rev. D **59**, 105006 (1999). hep-ph/9811350
22. E. Gabrielli, B. Mele, Nucl. Phys. B **647**, 319 (2002). hep-ph/0205099
23. B. Grinstein, C.W. Murphy, D. Pirtskhalava, P. Uttayarat, J. High Energy Phys. **1208**, 073 (2012). arXiv:1203.2183 [hep-ph]
24. N. Davidson, G. Nanava, T. Przedzinski, E. Richter-Was, Z. Was, Comput. Phys. Commun. **183**, 821–843 (2012). 1002.0543
25. S. Alioli, P. Nason, C. Oleari, E. Re, J. High Energy Phys. **0904**, 002 (2009). arXiv:0812.0578 [hep-ph]
26. P. Nason, C. Oleari, J. High Energy Phys. **1002**, 037 (2010). arXiv:0911.5299 [hep-ph]
27. S. Dittmaier et al. (LHC Higgs Cross Section Working Group), arXiv:1101.0593 [hep-ph]
28. S. Dittmaier et al. (LHC Higgs Cross Section Working Group), arXiv:1201.3084 [hep-ph]
29. Z. Was, S. Jadach, Phys. Rev. D **41**, 1425 (1990)
30. R.K. Ellis, I. Hinchliffe, M. Soldate, J.J. van der Bij, Nucl. Phys. B **297**, 221 (1988)
31. A. Elagin, P. Murat, A. Pranko, A. Safonov, Nucl. Instrum. Methods A **654**, 481–489 (2011). arXiv:1012.4686 [hep-ex]
32. D.L. Rainwater, D. Zeppenfeld, K. Hagiwara, Phys. Rev. D **59**, 014037 (1998). hep-ph/9808468
33. T. Plehn, D.L. Rainwater, D. Zeppenfeld, Phys. Rev. D **61**, 093005 (2000). hep-ph/9911385
34. LCG project. http://sftweb.cern.ch/generators/http://lcg.web.cern.ch/LCG/
35. M. Kirsanov, A. Ribon, O. Zenin, in *PoS ACAT08* (2008), p. 114. See also http://lcgapp.cern.ch/project/simu/generator/